

Implementation of a Method for Reconstructing Broadband Dielectric Properties

Fakultät für Physik und Geowissenschaften
Universität Leipzig

Bachelor Arbeit

Jan Zimbelmann

Matrikelnummer: 3675087

Universität Leipzig
Prof. Dr. rer. nat. habil. Jan Meijer

Helmholtz-Zentrum für Umweltforschung - UFZ
Dr.-Ing. Jan Bumberger

Leipzig, May 31, 2019

Contents

1	Introduction	1
2	Theory	2
2.1	Dielectric Permittivity	2
2.2	Derivation of the Telegrapher's Equations	3
2.3	Simulation with Qucs	5
2.3.1	Qucs Simulation Results	6
2.4	Analytic Method	7
2.4.1	Simulation of the S-Parameters (Forward Model)	7
2.4.2	Reconstruction of the Permittivity (Inversion Model)	10
2.4.3	Application of both Previous Methods	11
3	Measurement and Evaluation	16
3.1	Measuring Setup	16
3.1.1	Calibration	17
3.2	Evaluation	18
3.2.1	PTFE (Polytetrafluorethylen)	19
3.2.2	PE (Polyethylen)	22
3.2.3	PVDF (Polyvinylidenfluorid)	25
4	Conclusion and Future Applications	28
5	Appendix	29
5.1	Code for the Forward Model	29
5.2	Code for the Inverse Model	31
References		33

Abbreviations

S-parameters	Scattering Parameters
Qucs	Quite Universal Circuit Simulator
VNA	Vector Network Analyzer
RLGC	Resistance, Inductance, Conductance and Capacitance
DUT	Device Under Test
ECal Kit	Electronic Calibration Kit
NIST	National Institute of Standards and Technology
PTB	Physikalisch-Technische Bundesanstalt
PTFE	Polytetrafluorethylen
PE	Polyethylen
PVDF	Polyvinylidenfluorid

1 Introduction

In this Bachelor thesis I present to you methods for a broadband frequency permittivity reconstruction. My scope of interest is to look at a coaxial assembly and to derive the permittivity from the Scattering parameters (S-parameters) in a broadband frequency range. This includes to look at the S-parameters from a real life measuring setup, an analytic calculation as well as a software circuit simulator. The software of choice for this is Qucs (Quite Universal Circuit Simulator). There is also a theoretical part for explaining dielectric spectroscopy in a basic way.

In a two port measuring constellation with a vector network analyzer (VNA) there are two sources for a signal to propagate. In this case there are four S-parameters: S_{11} , S_{12} , S_{21} , S_{22} . The two S-parameters with the same indices are characterizing how much of the signal is reflected back to the emitting source. Those are the reflective S-parameters. The two parameters with different indices are defining the fraction of the signal which passes to the other port. Those are the transmitting S-parameters. The VNA can measure this set of S-parameters. The method for reconstructing the permittivity is an analytic method which can be derived from the telegrapher's equation and the propagation matrices. This method is able to reconstruct the real and imaginary part of the relative permittivity in the case for a homogeneous single layer setup as well as producing the S-parameter set for any amount of homogeneous layers. The implementation of the algorithm in this thesis simulates different single layer sets of S-parameters with a selected permittivity behavior and reconstructs the permittivity of them. Furthermore it reconstructs the permittivity of measured S-parameters.

In this real life application for generating a set of S-parameter results, there is the coaxial cell which consists of two in each other placed copper pipes. Between those two copper pipes there is a dielectric placed. Now the real and imaginary part of the relative permittivity is to be reconstructed. The dielectrics which had been measured are: PTFE, PE and PVDF. Two of which (PTFE and PE) show a constant real part of the relative permittivity in the measured frequency range. They also show low-losses properties. Therefore for those two materials a low imaginary permittivity is to be expected. The analytic simulation for the real life application can be compared to the literature values for those two measurements.

2 Theory

In this section the behavior of a electric signal propagating through a multiple layer setup is discussed. This behavior is described by the telegrapher's equations. Moreover there is a method explaining the reconstruction the the permittivity according to a propagation matrices model. There are two ways presented to construct a set of S-parameters with a chosen permittivity and the reconstruction of the permittivity is tested on those methods. But firstly there is a groundwork on how to understand what a dielectric permittivity stands for.

2.1 Dielectric Permittivity

For a Dielectric in an electric field, electric charges in the material do not flow according to the potential difference as it would happen in a conductor but instead shift from their equilibrium state. This results in a polarization in which the positive charges are attracted towards and the negative charges contrary to the electric field. Due to this arrangement the electric field within the material is reduced. The dielectric permittivity ϵ is a property which describes the degree of electric polarization of the material in a electric field. For a linear, homogeneous and isotropic material and assuming a instantaneous response to a change in the electric field, there is the following relation between the electric field \mathbf{E} and the electric disposal field \mathbf{D} [1, p. 23]:

$$\mathbf{E} = \epsilon \mathbf{D} \quad (1)$$

The permittivity consists of the electric permittivity of free space ϵ_0 and the relative permittivity ϵ_r :

$$\epsilon = \epsilon_0 \epsilon_r \quad (2)$$

Permittivity is not characterized by a constant. It depends on many parameters such as the temperature, the position in the medium, humidity and more. For this study however the important dependency is: how does the permittivity change in a changing electric field? Therefore the frequency dependency in particular is1 interesting:

$$\epsilon = \epsilon(f) \quad (3)$$

When observing the response of a material to an external field, the polarization in the material is not happening instantaneously. This response happens as a consequence to the change of the electric field and therefore can be represented with a phase difference. For a continuously changing electric field which is defined by a frequency f , the polarization in the material is trailing behind the polarization of the outer field. For this phase difference the permittivity is generally a complex number [2, p. 2 ff.]:

$$\epsilon_r = \epsilon'_r + i\epsilon''_r \quad (4)$$

This does not apply for vacuum. Since there is no matter to be polarized in vacuum there can be no phase difference in the polarization. Therefore the imaginary part of the relative permittivity of vacuum equals zero. Since the real part of the relative permittivity is a multiplier according to the permittivity in vaccum, the real part of the relative permittivity in vacuum is 1.

2.2 Derivation of the Telegrapher's Equations

A conductor in an electric circuit does not have a perfect conducting performance. A transmission line is described by a distributed element model which assumes an infinite amount of infinitesimally small circuit elements [3, p. 6 ff.]. It consists of: resistance-, inductance-, conductance- and capacitance- elements (RLGC), distributed throughout the conductor. This also applies to the coaxial cell and leads to an impedance. For the wavelength of a signal to approach closer to a value of physical dimensions, the impedance of the coaxial cell starts to play a role in the transmission performance and cannot be neglected.

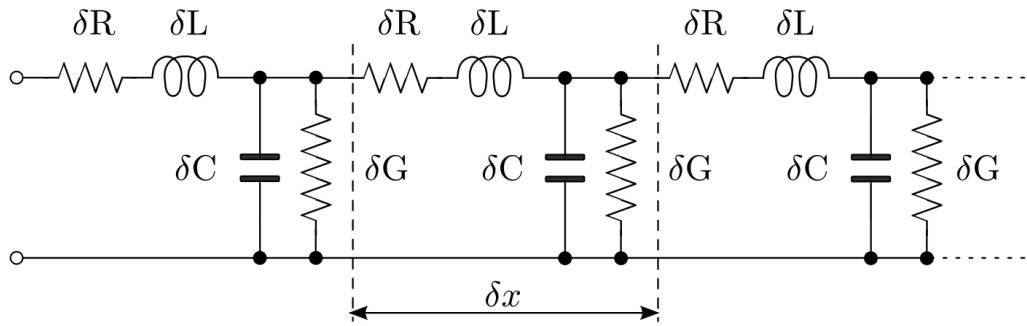


Fig. 1: Equivalent representation of a transmission line with an RLGC circuit. [4]

Voltage and current are derived by the well known electrical laws:

$$U = RI \quad (5)$$

$$U = L\dot{I} \quad (6)$$

$$G = 1/R \rightarrow I = GU \quad (7)$$

$$C = Q/U \rightarrow I = C\dot{U} \quad (8)$$

The wave equations are derived by utilizing the Kirchhoff's circuit laws for voltage and current. It is looked at a infinitesimally small part of the setup. Therefore all units: R , L , G , C are representing their property per length. Also Δx converges to 0 for a limes assumption.

Looking at the voltage:

$$u(x, t) - R\Delta x \cdot i(x, t) - L\Delta x \cdot \dot{i}(x, t) - u(x + \Delta x, t) = 0 \quad (9)$$

$$\lim_{\Delta x \rightarrow 0} \frac{u(x, t) - u(x + \Delta x, t)}{\Delta x} = Ri(x, t) + L\dot{i}(x, t) \quad (10)$$

$$\frac{\partial u(x, t)}{\partial x} = Ri(x, t) + L\dot{i}(x, t) \quad (11)$$

Looking at the current:

$$i(x, t) - G\Delta x \cdot u(x, t) - C\Delta x \cdot \dot{u}(x, t) - i(x + \Delta x, t) = 0 \quad (12)$$

$$\lim_{\Delta x \rightarrow 0} \frac{i(x, t) - i(x + \Delta x, t)}{\Delta x} = Ru(x, t) + C\dot{u}(x, t) \quad (13)$$

$$\frac{\partial i(x, t)}{\partial x} = Ru(x, t) + C\dot{u}(x, t) \quad (14)$$

The time dependency of the current i and voltage u is assumed to be harmonic. To simplifying the equations (11) and (14) a cosine phasor is implemented [5, p. 9-11].

$$\begin{aligned} u(x, t) &= \hat{u}(x) \cdot \cos(\omega t + \phi(x)) = \operatorname{Re} \left(u(x) e^{j\omega t} \right) \\ u(x) &= \hat{u}(x) \cdot \exp(j\phi(x)) \end{aligned} \quad (15)$$

Now the voltage and current are represented time invariant. This is displayed by changing the voltage and current from the italic written u and i to the normal written letters u and i .

$$\frac{du}{dx} = -i(x) \cdot (R + j\omega L) \quad (16)$$

$$\frac{di}{dx} = -u(x) \cdot (G + j\omega C) \quad (17)$$

Now there is another differentiation of the equation (16) and the complex propagation constant γ is introduced.

$$\frac{d^2u(x)}{dx^2} = -(R + j\omega L) \cdot \frac{di(x)}{dx} = (R + j\omega L)(G + j\omega C) \cdot u(x) \quad (18)$$

$$\gamma = \sqrt{(R + j\omega L)(G + j\omega C)} \quad (19)$$

Furthermore one obtains the following differential equations:

$$\frac{d^2u(x)}{dx^2} - \gamma^2 u(x) = 0 \quad (20)$$

$$\frac{d^2i(x)}{dx^2} - \gamma^2 i(x) = 0 \quad (21)$$

Solving these harmonic equation gives the desired wave equation for u :

$$u(x) = u_0^+(x) \cdot \exp(-\gamma x) + u_0^-(x) \cdot \exp(\gamma x) \quad (22)$$

When inserting equation (22) into (16) and solving for the current i , it gets to:

$$i(x) = \frac{\gamma}{R + j\omega L} \left(u_0^+(x) \cdot \exp(-\gamma x) + u_0^-(x) \cdot \exp(\gamma x) \right) \quad (23)$$

Finally the characteristic impedance Z_W for a new expression of the current i is implemented:

$$Z_W = \frac{R + j\omega L}{\gamma} = \sqrt{\frac{R + j\omega L}{G + j\omega C}} \quad (24)$$

$$i(x) = \frac{1}{Z_W} \left(u_0^+(x) \cdot \exp(-\gamma x) + u_0^-(x) \cdot \exp(\gamma x) \right) \quad (25)$$

2.3 Simulation with Qucs

The goal of the simulation in Qucs (version 0.0.19) is to create a first set of S-parameters for which the permittivity can be reconstructed. In the real life application a Network analyzer is used to generate two signals from two ports. Therefore two power sources (P1 and P2) are used in the simulation. The frequency range is set from 300 kHz to 3.4 GHz with 1601 measurement points. This boundary conditions are equivalent to those of the real life settings. 'D' equates to the outer diameter of the shield, 'd' to the inner diameter of the conductor and 'L' is the length of the coaxial cell. The relative permittivity is set constant for all frequency points to 2.1. The synthetic material PTFE also has a similar property, a constant real part of the relative permittivity of 2.1 in the GHz range as well as a very low imaginary part. PTFE is one of the devices under test (DUT) in the real life application.

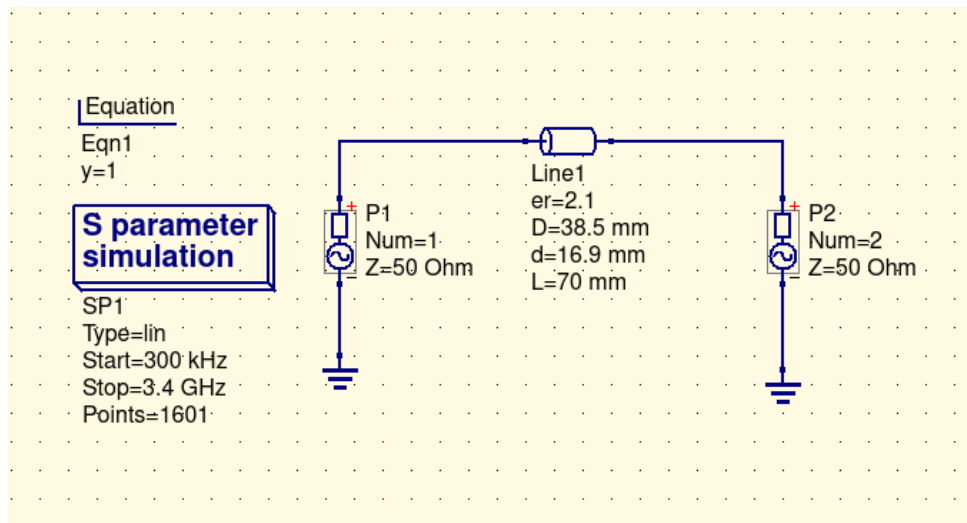


Fig. 2: Qucs simulation for the S-parameters of a coaxial cell. The signal frequency sweeps in a range from 300 kHz to 3.4 GHz.

2.3.1 Qucs Simulation Results

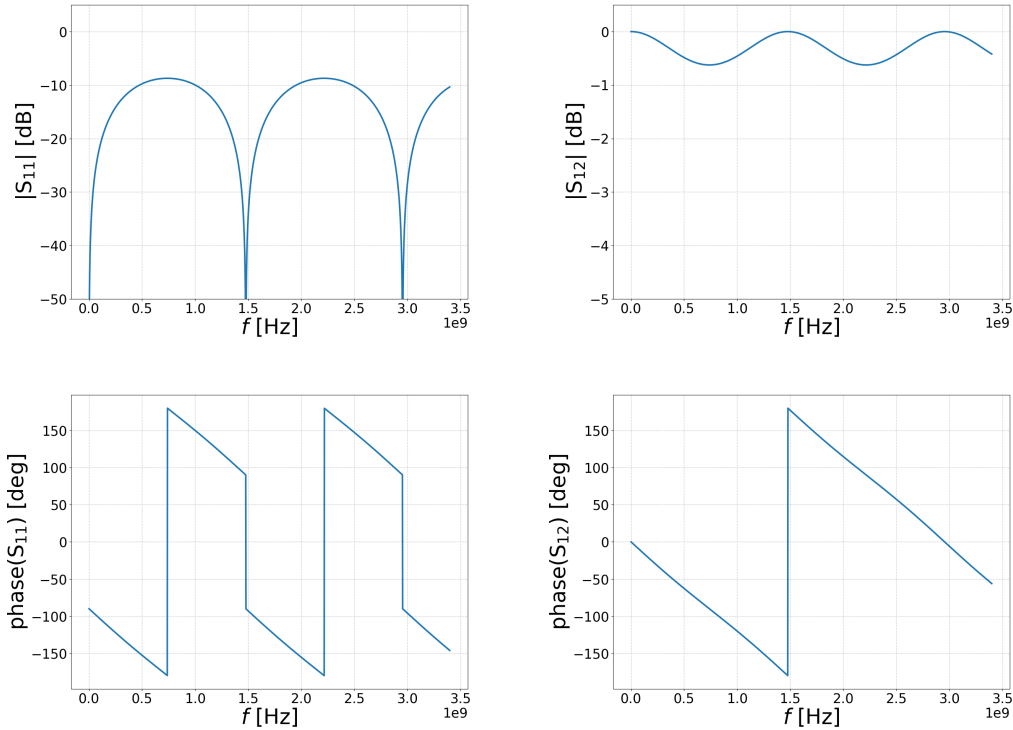


Fig. 3: Results of the simulation in Qucs. The boundary conditions are visible in figure 2. The reflecting S-parameters are identical and therefore just the S_{11} parameter is shown. This also applies to the transmitting S-parameters and S_{12} . They are displayed in absolute and phase.

The results in figure 3 show the absolutes of the S_{11} and S_{12} parameters as well as their phases. For both, the absolute and the phase. The S_{11} parameter is equivalent to the S_{22} parameter. This also applies for the two transmitting S-parameters and therefore only one of each is shown in the graph. The behavior of the curve appears harmonic and periodic. This is because there is no losses calculated in the simulation. In a later chapter this constant relative permittivity is reconstructed.

2.4 Analytic Method

The technique presented for reconstructing the frequency dependent permittivity is derived from the paper: 'A New Tool for Accurate S-Parameters Measurements and Permittivity Reconstruction' [6, p. 3-6]. The measuring assembly is a multiple layered setup with different properties for each of the layers. Those properties vary in the geometry and dielectric characteristics. The layer of interest however is the one with the DUT. Due to a calibration all the other layers length get corrected to a length of zero.

This method enables to either simulate the S-parameters (forward model) or to utilize the four parameters to reconstruct dielectric properties (inverse model). In the following sections both methods are presented and the results are shown to work recursively.

2.4.1 Simulation of the S-Parameters (Forward Model)

The measuring setup is separated into multiple layers. In the middle there is the sample holder with the dielectric material and to the left and right are the cables, adapters and the ports of the VNA. The propagation of the signal is described by propagation matrices for each of the layers.

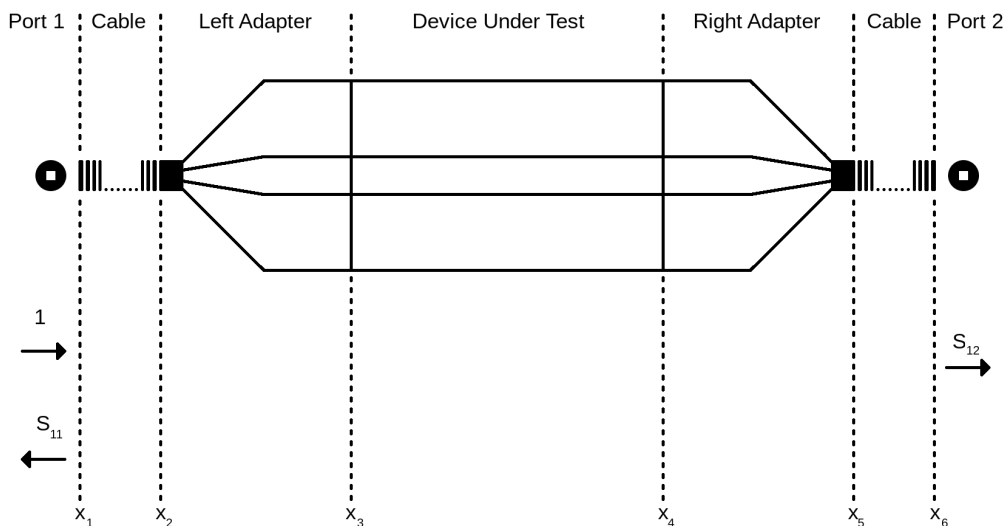


Fig. 4: Representation of the multiple sections of the measurement setup with the amplitudes of a propagating electromagnetic wave.

The wave functions are described in the equation [22] given for each of the layers. Now the equation is represented in down going and up coming wave field within the layer n . Both terms of the sum are stating the different position and direction from which and where the wave occurs and propagates.

$$\mathbf{V}_n(z) = \begin{bmatrix} V_n^+ \\ V_n^- \end{bmatrix} \quad (26)$$

$$V_n = V_n^+ \cdot e^{-\gamma(x-x_{n-1})} + V_n^- \cdot e^{-\gamma(x_n-x)} \quad (27)$$

$$I_n = \frac{1}{Z_n} \left[V_n^+ \cdot e^{-\gamma(x-x_{n-1})} - V_n^- \cdot e^{-\gamma(x_n-x)} \right] \quad (28)$$

The propagation matrices are introduced with the following definition from the paper [6, p. 3].

$$\mathbf{M}_n^L \mathbf{V}_n = \mathbf{M}_{n+1}^R \mathbf{V}_{n+1} \quad (29)$$

With:

$$\mathbf{M}_n^L = \begin{bmatrix} e^{-\gamma_n l_n}, & 1 \\ \frac{1}{Z_n}, & \frac{1}{Z_n} e^{-\gamma_n l_n} \end{bmatrix} \quad (30)$$

$$\mathbf{M}_n^R = \begin{bmatrix} 1, & e^{-\gamma_n l_n} \\ \frac{1}{Z_n} e^{-\gamma_n l_n}, & \frac{1}{Z_n} \end{bmatrix} \quad (31)$$

The propagation of the wave function is now considered from port 1 to the port 2. The propagation matrices in this form enable to relate the field of the very first interface to the very last interface with the following relationship:

$$\mathbf{V}_1 = (\mathbf{M}_1^L)^{-1} \left(\prod_{n=2}^{N-1} \mathbf{M}_n^R (\mathbf{M}_n^L)^{-1} \right) \mathbf{M}_N^R \mathbf{V}_N \quad (32)$$

Looking at the right side of the equation (32), the term before \mathbf{V}_N can be divided into three expressions. \mathbf{P} is representing the propagation matrices for the DUT. \mathbf{L} are the matrices to the left and \mathbf{R} are those to the right of the DUT:

$$\mathbf{P} = \mathbf{M}_p^R (\mathbf{M}_p^L)^{-1} \quad (33)$$

$$\mathbf{L} = (\mathbf{M}_1^L)^{-1} \left(\prod_{n=2}^{n=p-1} \mathbf{M}_n^R (\mathbf{M}_n^L)^{-1} \right) \quad (34)$$

$$\mathbf{R} = \left(\prod_{n=p+1}^{n=N-1} \mathbf{M}_n^R (\mathbf{M}_n^L)^{-1} \right) \mathbf{M}_N^R \quad (35)$$

The equation (32) can now be rewritten by considering the implementation of \mathbf{L} , \mathbf{R} and \mathbf{P} :

$$\mathbf{V}_1 = \mathbf{L} \mathbf{P} \mathbf{R} \mathbf{V}_N \quad (36)$$

When the calibration is considered, like in the real life experiment, \mathbf{L} and \mathbf{R} can be simplified. Due to the calibration the length of the layers to the left and right of the sample holder are set to zero ($l_n = 0$ for $n \neq p$):

$$\mathbf{L} = \begin{bmatrix} 1, & 1 \\ \frac{1}{Z_0}, & -\frac{1}{Z_0} \end{bmatrix}^{-1} \quad (37)$$

$$\mathbf{R} = \begin{bmatrix} 1, & 1 \\ \frac{1}{Z_0}, & -\frac{1}{Z_0} \end{bmatrix} \quad (38)$$

The characteristic impedance for the network analyzer used in the experiment is defined by 50Ω . \mathbf{P} can be displayed as such:

$$\mathbf{P} = \begin{bmatrix} \cosh(l_p \cdot \gamma_p), & Z_p \sinh(l_p \cdot \gamma_p) \\ \frac{\sinh(l_p \cdot \gamma_p)}{Z_p}, & \cosh(l_p \cdot \gamma_p) \end{bmatrix} \quad (39)$$

\mathbf{V}_1 and \mathbf{V}_N are both related to the S-parameters for the wave propagating from port 1 as visualized in figure 4. V_1^+ represents the wave propagating from port 1. V_1^- is the reflected part of the signal (S_{11}) and V_N^+ the propagating part (S_{12}). The propagation of the signal from port 1 is only considered here, therefore V_N^- is 0. Taking this into consideration (36) can be written as:

$$\begin{bmatrix} 1 \\ S_{11} \end{bmatrix} = \mathbf{L} \mathbf{P} \mathbf{R} \begin{bmatrix} S_{12} \\ 0 \end{bmatrix} \quad (40)$$

Now applied to the previous assumptions in (39). With \mathbf{L} to be the reciprocal of \mathbf{R} , they both will cancel each other and are therefore not shown:

$$\begin{bmatrix} 1 \\ S_{11} \end{bmatrix} = \mathbf{P} \begin{bmatrix} S_{12} \\ 0 \end{bmatrix} = \begin{bmatrix} \cosh(l_p \cdot \gamma_p), & Z_p \sinh(l_p \cdot \gamma_p) \\ \frac{\sinh(l_p \cdot \gamma_p)}{Z_p}, & \cosh(l_p \cdot \gamma_p) \end{bmatrix} \begin{bmatrix} S_{12} \\ 0 \end{bmatrix} \quad (41)$$

When solving the formula (41) for S_{11} and S_{12} this relations are obtained:

$$S_{12} = P_{11} = \cosh(l_p \cdot \gamma_p) \quad (42)$$

$$S_{11} = \frac{P_{21}}{P_{11}} = \frac{\sinh(l_p \cdot \gamma_p)}{Z_p \cdot \cosh(l_p \cdot \gamma_p)} \quad (43)$$

Since the arrangement is symmetrical, the transmission and propagation behavior of the second port can be identified with the one from the first port. Therefore S_{22} equals to S_{11} and S_{21} to S_{12} . The characteristic impedance Z_p and the propagation factor γ_p is described in the paper [6, p. 6].

$$Z_p = Z_0 \sqrt{\frac{\epsilon_r}{\mu_r}} \quad (44)$$

$$\gamma_p = \sqrt{\epsilon_r \mu_r} \frac{j\omega}{c_0} \quad (45)$$

2.4.2 Reconstruction of the Permittivity (Inversion Model)

This section discovers how to reconstruct the relative permittivity from a set of S-parameters with a similar propagation matrices terminology. \mathbf{P} is described in formula (39). The equation (36) is now rewritten in another convenient form:

$$\begin{bmatrix} A \\ B \end{bmatrix} = \mathbf{P} \begin{bmatrix} C \\ D \end{bmatrix} \quad (46)$$

With the following relation when comparing (46) to (40), A, B, C and D can be described with:

$$\begin{bmatrix} A \\ B \end{bmatrix} = \mathbf{L}^{-1} \begin{bmatrix} 1 \\ S_{11} \end{bmatrix} \quad (47)$$

$$\begin{bmatrix} C \\ D \end{bmatrix} = \mathbf{R} \begin{bmatrix} S_{12} \\ 0 \end{bmatrix} \quad (48)$$

When having the formulas (47) and (48) solved for the individual parameters:

$$A = 1 + S_{11} \quad (49)$$

$$B = \frac{1 - S_{11}}{Z_0} \quad (50)$$

$$C = S_{12} \quad (51)$$

$$D = \frac{S_{12}}{Z_0} \quad (52)$$

For \mathbf{P} taken from the equation (39) substituted into (46) it shows an expression for a reconstructed impedance when eliminating the exponential terms:

$$Z_p = \sqrt{\frac{A^2 - C^2}{B^2 - D^2}} \quad (53)$$

When instead eliminating the impedance terms in the substitution, a formula for the propagation constant γ_p is obtained:

$$\gamma_p = \frac{1}{l_p} \cdot \text{acosh}(\beta) \quad (54)$$

$$\beta = \left(\frac{A \cdot B + C \cdot D}{A \cdot D + B \cdot C} \right) \quad (55)$$

Finally when rearranging the equation (45) an expression for the reconstructed relative permittivity of the sample is given by:

$$\epsilon_r = \left(\frac{c_0 \cdot \gamma_p}{j \cdot \omega} \right)^2 \cdot \frac{1}{\mu_r} \quad (56)$$

The relative permeability μ_r is very close to 1 for non-magnetic materials.

2.4.3 Application of both Previous Methods

The methods in the previous chapters enable to create a set of S-parameters and to reconstruct the assumptions made for the permittivity. For the first analytic simulation the same boundary conditions are applied as in the qucs simulation (figure 2). The length of the line corresponds to 70 mm and the real part of the relative permittivity is set constant to a value of 2.1. The imaginary part of the relative permittivity is set at 0.0001.

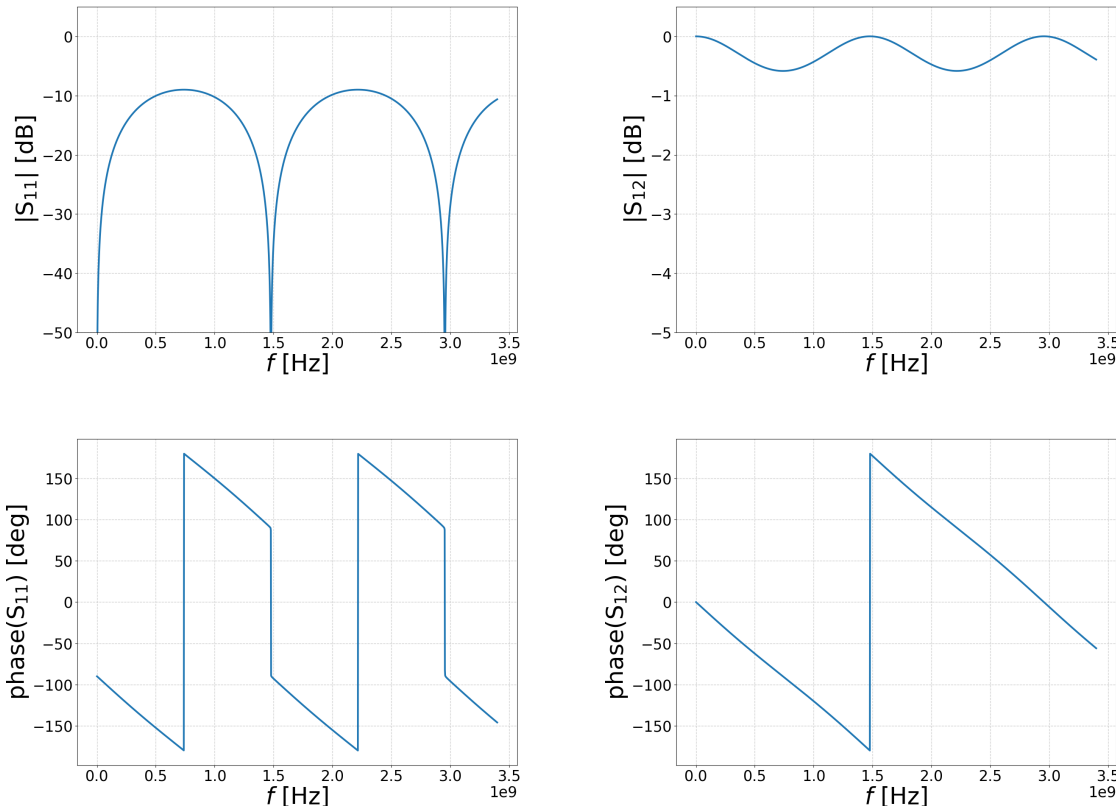


Fig. 5: Analytic simulation of the absolutes and phases for the S_{11} and S_{12} parameters according to the forward model method. The frequency range is set from 300 kHz to 3.4 GHz. Relative permittivity ϵ_r is set to $2.1 + 1e-4 i$ and the length l_p to 70 mm. Z_0 is set to 50Ω .

The results in the forward model (figure 5) are very similar to the results of the simulation with qucs (figure 2). This is to be expected when considering very similar boundary conditions for the two simulations.

Now the inverse model is used to reconstruct the relative permittivity with the S-parameter data sets which are displayed in figure 5 (forward model) and in figure 3 (simulation in qucs):

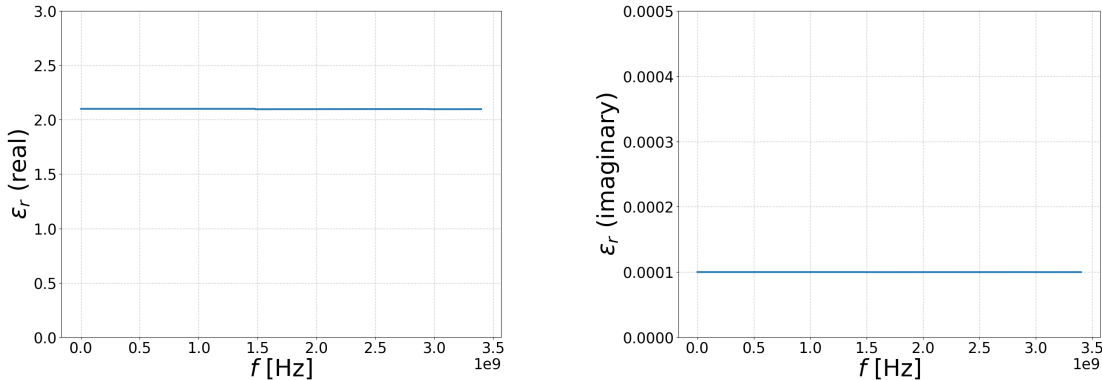


Fig. 6: Reconstruction of the relative frequency dependent permittivity ϵ_r according to the analytic inverse model. The S-Parameters taken into computation are those in the forward model, figure 5.

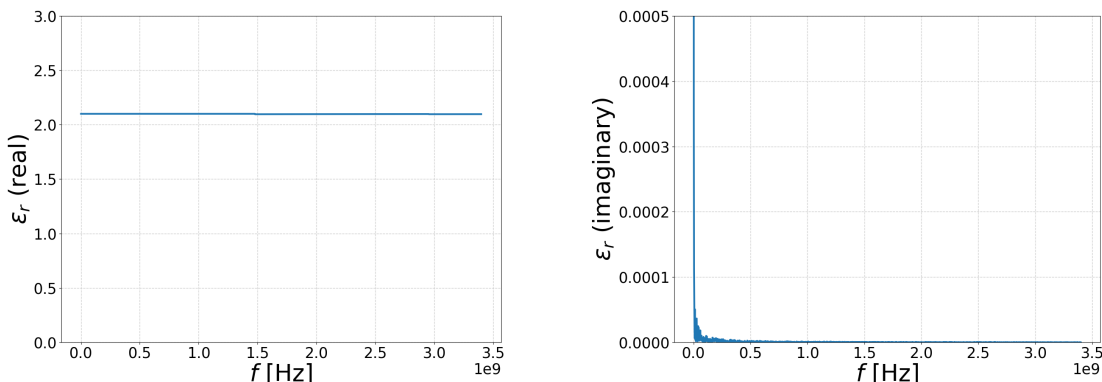


Fig. 7: Reconstruction of the relative frequency dependent permittivity ϵ_r according to the inverse model. The S-Parameters taken into computation are those from the simulation with qucs, figure 3.

The reconstruction of both sets of S-parameters (figure 6 and figure 7) show the real part of relative permittivity of 2.1 for the entire frequency range. This is the same value used to generate the set of S-parameters. The analytic result show a constant imaginary part of the permittivity at 1e-4. This also aligns to the value used to generate this set of S-parameters. The qucs-simulation is showing here a neglectable noise for the imaginary part of the permittivity close to 0.

In another example there is a linear dependency for both: the imaginary and the real part of the relative permittivity. This is going to be a fictional material with a linear increasing real part of the relative permittivity from 2 to 5 and the imaginary part is linearly decreasing from 0.005 to 0. This is happening in the frequency range from 300 kHz to 3.4 GHz. With this set of S-parameters the inversion algorithm is once again applied for confirming its functionality in a non-linear case.

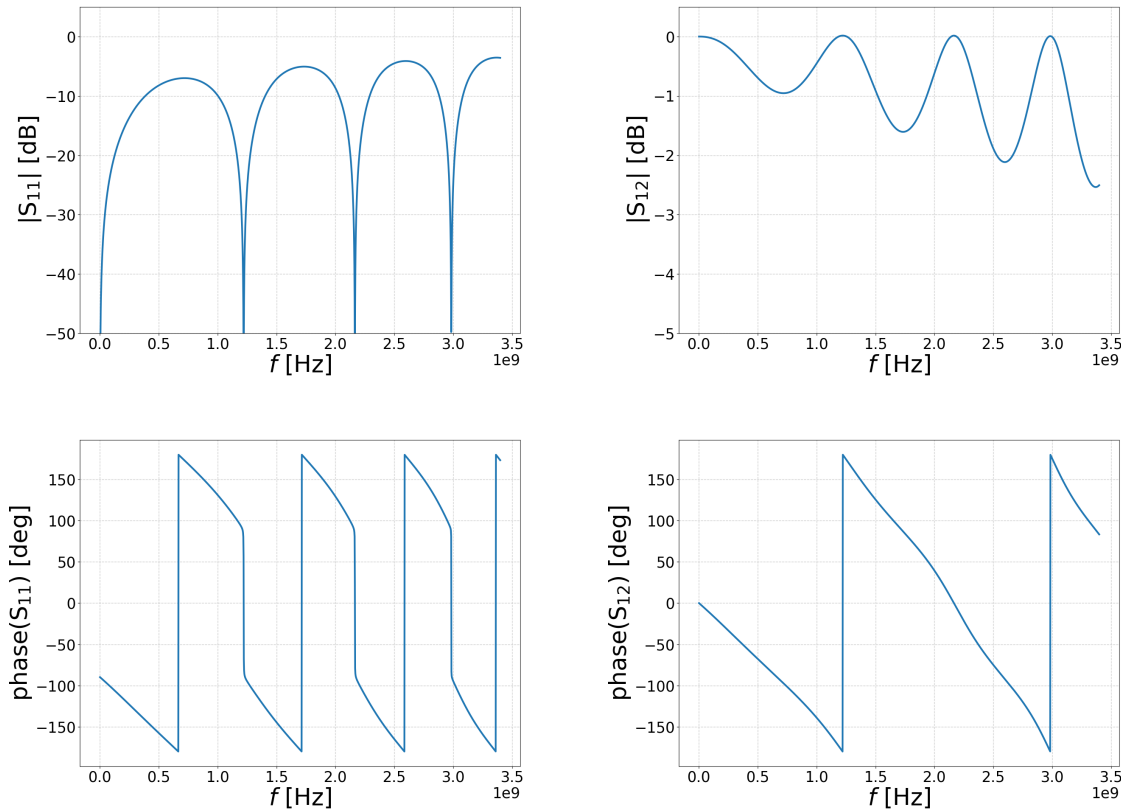


Fig. 8: Analytic simulation of S-parameters. Frequency range from 300 kHz to 3.4 GHz, linear increasing real part of the relative permittivity ϵ_r in the range from 2 to 5 and a imaginary part from 0.005 to 0. $l_p = 70$ mm. $Z_0 = 50 \Omega$.

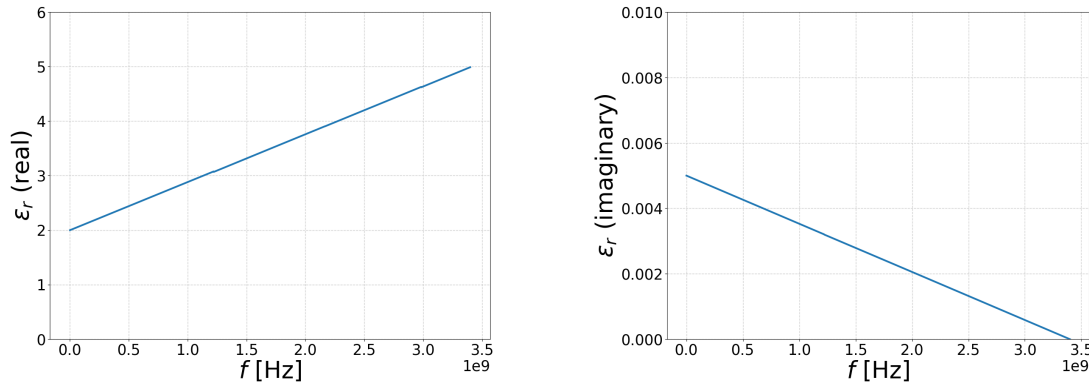


Fig. 9: Reconstruction of the relative frequency dependent permittivity ϵ_r with the S-parameters in figure 8.

The results of the reconstruction shows the behavior accordingly to the chosen permittivity behavior. Therefore the construction and reconstruction of the S-parameters in the analytic calculation appears to be consistent with each other.

For implementing the inverse model in a computational program, one needs to make two corrections for the imaginary part of the gamma term (54). The signum of the imaginary part is switching seemingly randomly from plus to minus. The first correction in place is preventing this behavior. Also the curve is periodically wrapped and needs to be unwrapped with another correcting algorithm. Without this correction, the functionality of reconstructing of the relative permittivity stops working after the first wrapping. After this two correction terms have been implemented for the imaginary part of the propagation constant γ , the permittivity does get reconstructed for the entire frequency range. The behavior before and after the correction is visible in this figure:

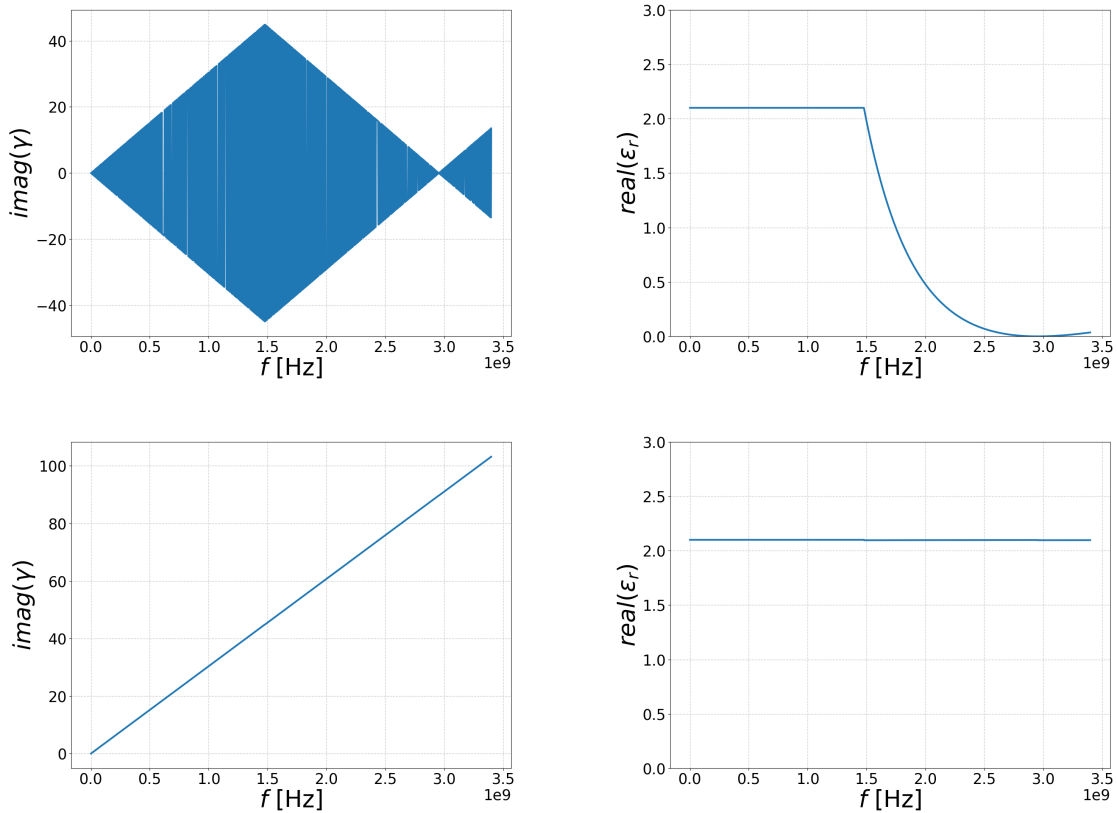


Fig. 10: Behavior of the relative permittivity of the S-parameters simulation with a constant $\epsilon_r = 2.1$ with different stages of correcting algorithms. The top two graphs represent the results without any correction for the imaginary part of γ . The bottom two graphs represent the results with the correction algorithm in place.

3 Measurement and Evaluation

This section deals with the real life application for generating a S-parameter set on a synthetic material. Moreover the permittivity is reconstructed and compared to literature values. But firstly the measuring setup and calibration is described.

3.1 Measuring Setup

Some boundary conditions for this particular measuring setup had already been mentioned in the sections about the simulations but are described here in detail once again.

The concept of this experiment is to measure the S-parameters having a dielectric of interest placed in the measuring setup. The S-parameters are measured with electromagnetic signals coming from and are also reflected back to the two ports of a vector network analyzer. The VNA used in this setup is an E5071C ENA Series Network Analyzer (Agilent Technologies). Each of the ports is connected with a phase stable cable to one of the two adapters. The adapters here are placed in a carrier on a railing system for more stable measuring circumstances. The adapter translates for the measures of the coaxial cell to the cables.

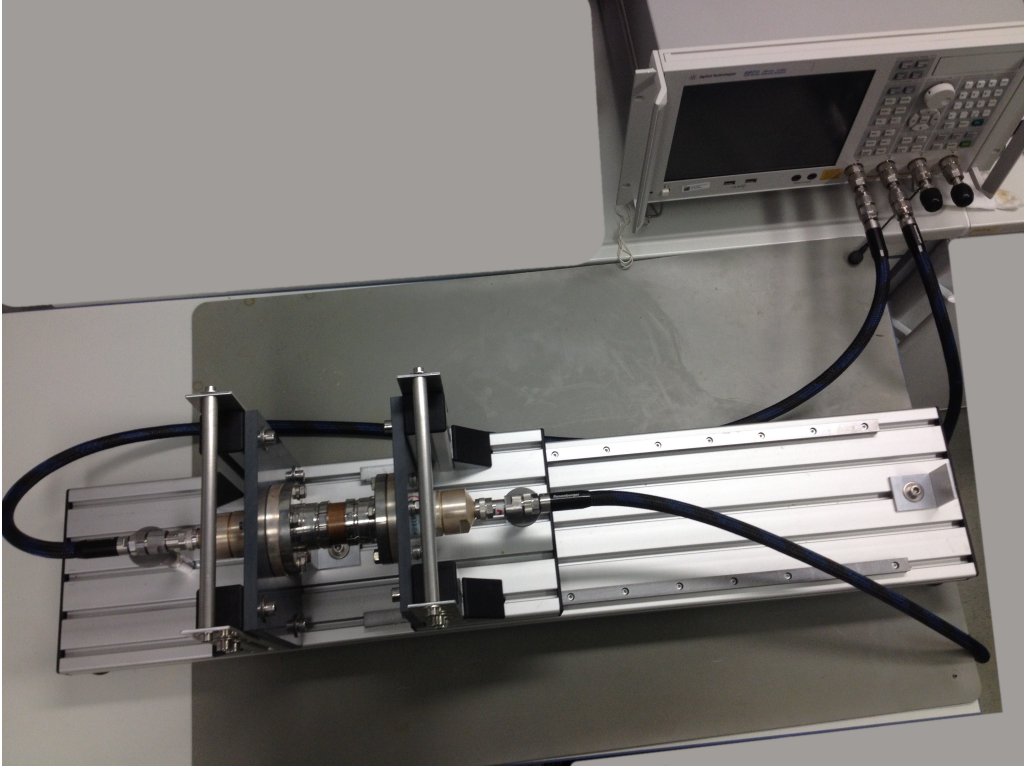


Fig. 11: Measuring setup. Phase stable cables are connecting the VNA to the adapters. The adapters hold the coaxial cell and the analyzed probe is within the coaxial cell.

The Coaxial cell consists of two into one another placed copper pipes. This is shown in the left picture of figure 12. A synthetic solid is placed within the coaxial cell. It is formed as a hollow cylinder with a 38.5 mm outer and a 16.9 mm inner diameter. This is shown in the right picture of the figure 12. The length of the copper pipes and synthetic materials are 70 mm.



Fig. 12: The empty coaxial cell is displayed in the left picture. The coaxial cell filled with a synthetic material (here: PTFE) is shown in the right picture.

3.1.1 Calibration

A calibration is necessary to firstly correct the systematic mistakes of the two port measurements in the network analyzer. The error sources are equivalent for both of the ports and include a behavior such as a reflection and a damping at the port or a phase delay of the signal transmission. Secondly it is necessary to reduce the measured S-parameters to the layer in which only the sample holder is considered. To achieve this goal two different calibrations are performed.

The first calibration is made within the VNA and utilizes a electronic calibration (ECal) kit [7, p. 16 ff.]. The ECal kit (N4431-60006 from Agilent Technologies, figure 13) is placed instead of the sample holders and adapters. Within the VNA it is then possible to perform this calibration. It corrects the systematic errors of the VNA and reduces the measured layers to the adapters and sample holders.



Fig. 13: anritsu calibration device for calibrating electrical.

The second calibration deals with correcting the two layers representing the adapters and reduces therefore the arrangement to a single layer problem. This is the layer which contains the DUT. The software used for this is the 'Statistical VNA Calibration Software Package' which is based on an algorithm developed at the 'National Institute of Standards and Technology' (NIST, United States) and the 'Physikalisch-Technische Bundesanstalt' (PTB, Germany). It is an iterative algorithm [8, p. 1] which calculates a correction for each of the frequency points in the measuring and is based on orthogonal distance regression. It can use different kinds of standards for calibrating the measuring setup.

The standards used in this calibrations are measurements with 'thru', 'line' and 'open' setups [8, p. 10]. The 'open' measuring implies the setup without the coaxial cell and measures the circuit with only air in between the two adapters. For this standard you would expect for the transmitting S-parameters S_{12} and S_{21} to realize a value of 0. The 'thru' setup assumes a zero length measurement. For this is a full transmission without any reflection expected. Therefore the reflecting S-parameters S_{11} and S_{22} are expected to reach a value of 1 and the the S_{12} and S_{21} to get a value of 0. The 'line' setup implies the coaxial cell without any dielectric in which the characteristic impedance of 50Ω is set to match the characteristic impedance of the empty coaxial cell.

3.2 Evaluation

The focus of this thesis is to develop a working algorithm for reconstructing the relative permittivity. Due to this priority I decided after multiple measurements by myself (in the year 2019) to take the S-parameter measurements by Felix Schmidt (scientist at the 'Helmholtz Zentrum für Umweltforschung GmbH - UFZ') from the 30th of January 2018. His measured data manage to show a very symmetrical behavior of the S-parameters.

3.2.1 PTFE (Polytetrafluorethylen)

PTFE is the first synthetic dielectric to be tested. It is 'generally accepted' [9, p. 4] for PTFE to have a constant relative permittivity of 2.1 in the GHz range. It is a low-losses material and therefore a low imaginary part of the relative permittivity is expected. PTFE is also known as Teflon.

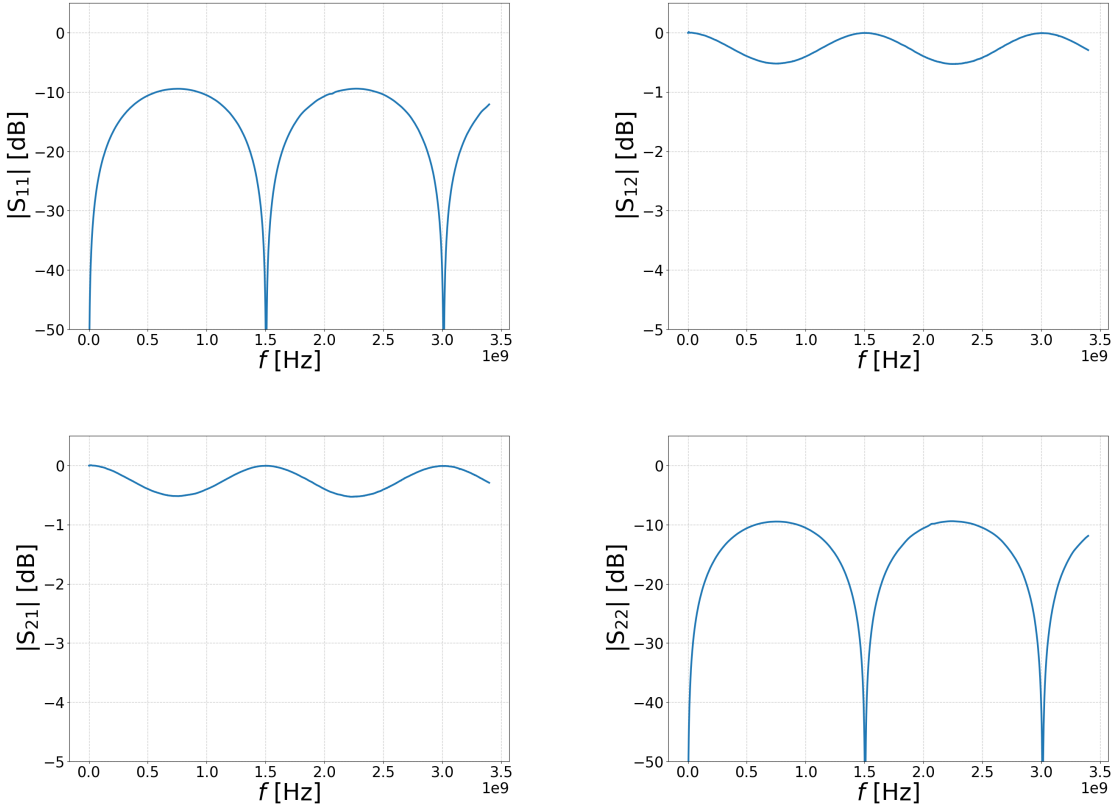


Fig. 14: Results of the absolutes of all S-parameters with the measurement with PTFE. The frequency range is set from 300 kHz to 3.4 GHz with 1601 data points.

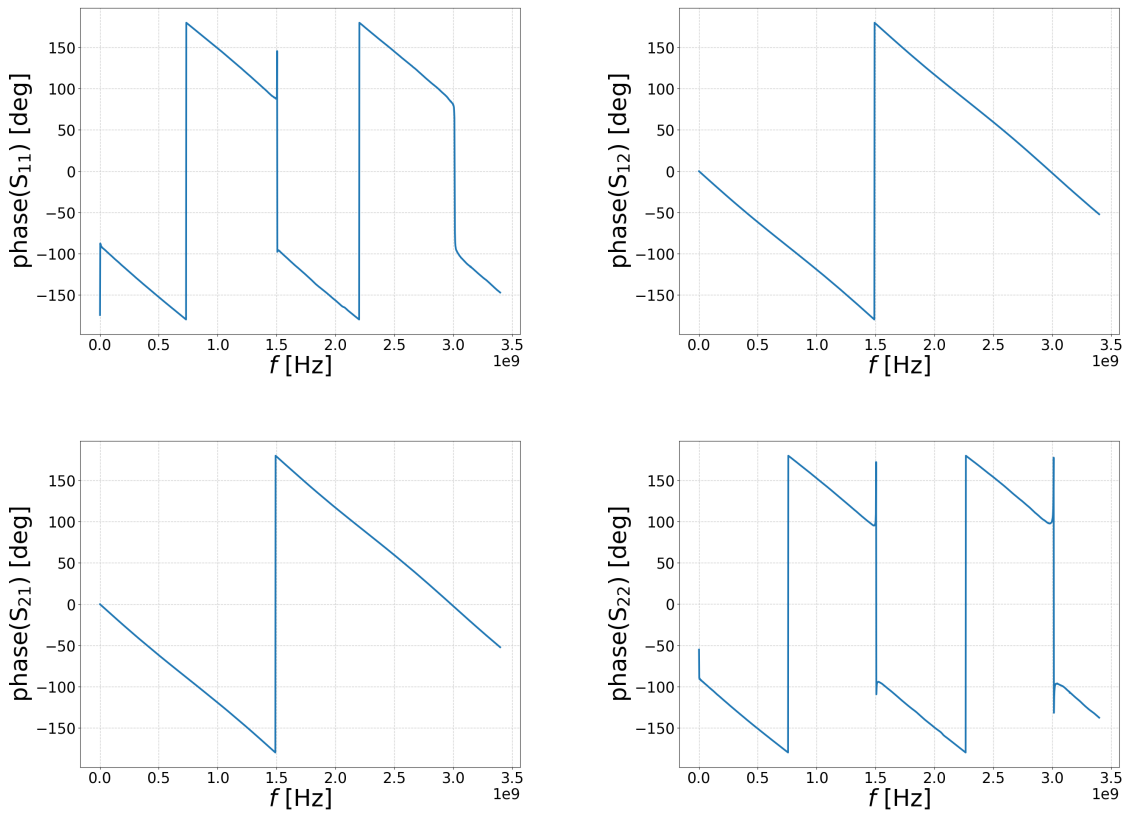


Fig. 15: Results of the phases of all the S-parameters with the measurement with PTFE. The frequency range is set from 300 kHz to 3.4 GHz with 1601 data points.

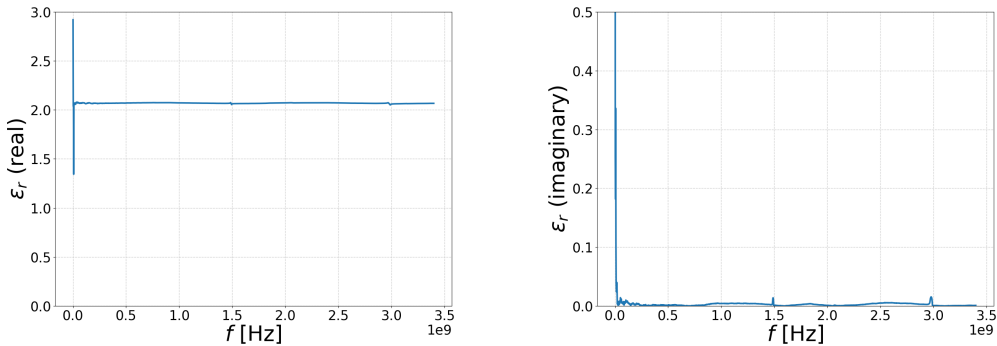


Fig. 16: Reconstruction of the relative permittivity with the S-parameters of PTFE which are shown in figure 14 and 15. The left graph shows the real part and right graph the imaginary part of the relative permittivity. The frequency span is as in the referring graphs from 300 kHz to 3.4 GHz.

This graphs show the absolute of the measured S-parameters (figure 14) and phase (figure 15) of PTFE. The transmitting S-parameters appear very symmetrical to each other as well as the reflecting parameters. In figure 16 there is the reconstruction of the permittivity given in real and imaginary part. As expected for the real part of the permittivity, it shows a very constant behavior close to 2.10. Since the real relative permittivity shows a constant behavior the idea of an averaging comes into consideration to enable a comparison of the results. For the averaging, the first 0.1 GHz is excluded because of the artifacts in this region. An average of 2.07 is calculated for the remaining frequency span. This however is not totally accurate to the expected permittivity but very close. However as for the imaginary part, the value goes close to zero, which is expected for a low-losses material.



Fig. 17: Picture of the PTFE probe which is measured in this section.

3.2.2 PE (Polyethylen)

PE is the most common synthetic found in the plastic industry. It is mainly used in packaging. For further testing purposes the relative permittivity is also be characterized by this Method. A relative permittivity of 2.26 [9, p. 4] for the entire frequency range is expected and PE is also a low-loss material.

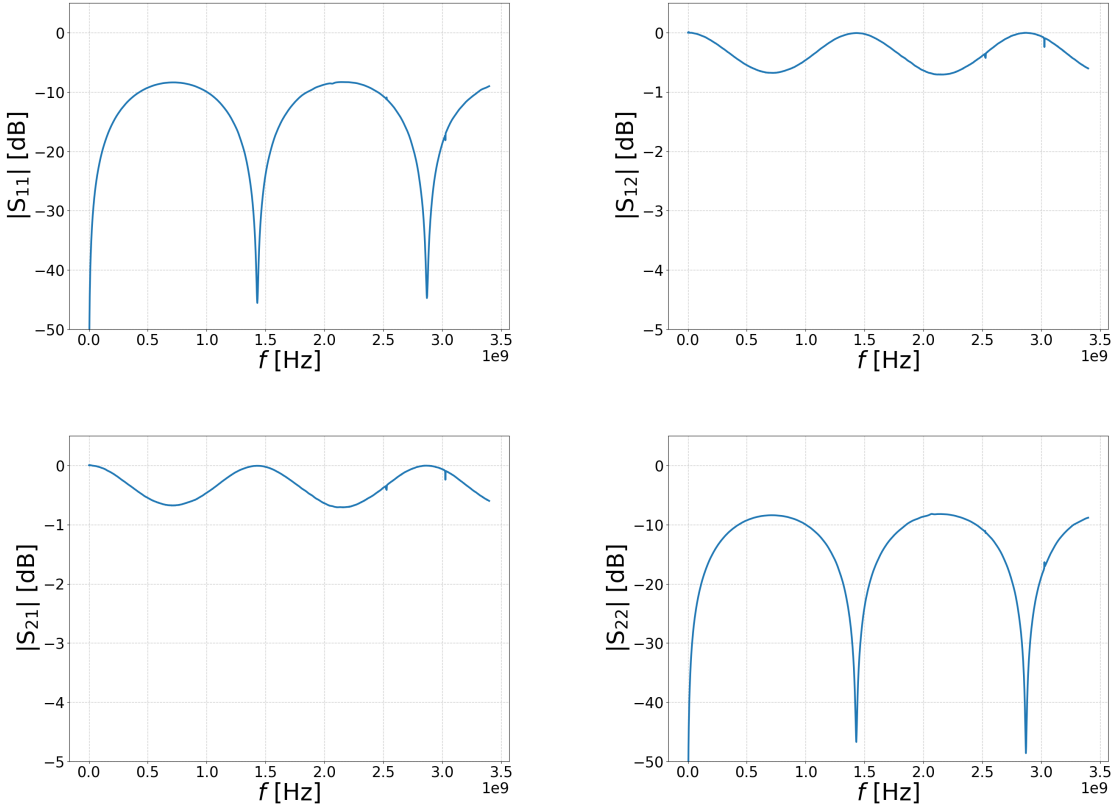


Fig. 18: Results of the absolutes of all S-parameters with the PE being measured in the sample holder. The frequency range is set from 300 kHz to 3.4 GHz with 1601 data points.

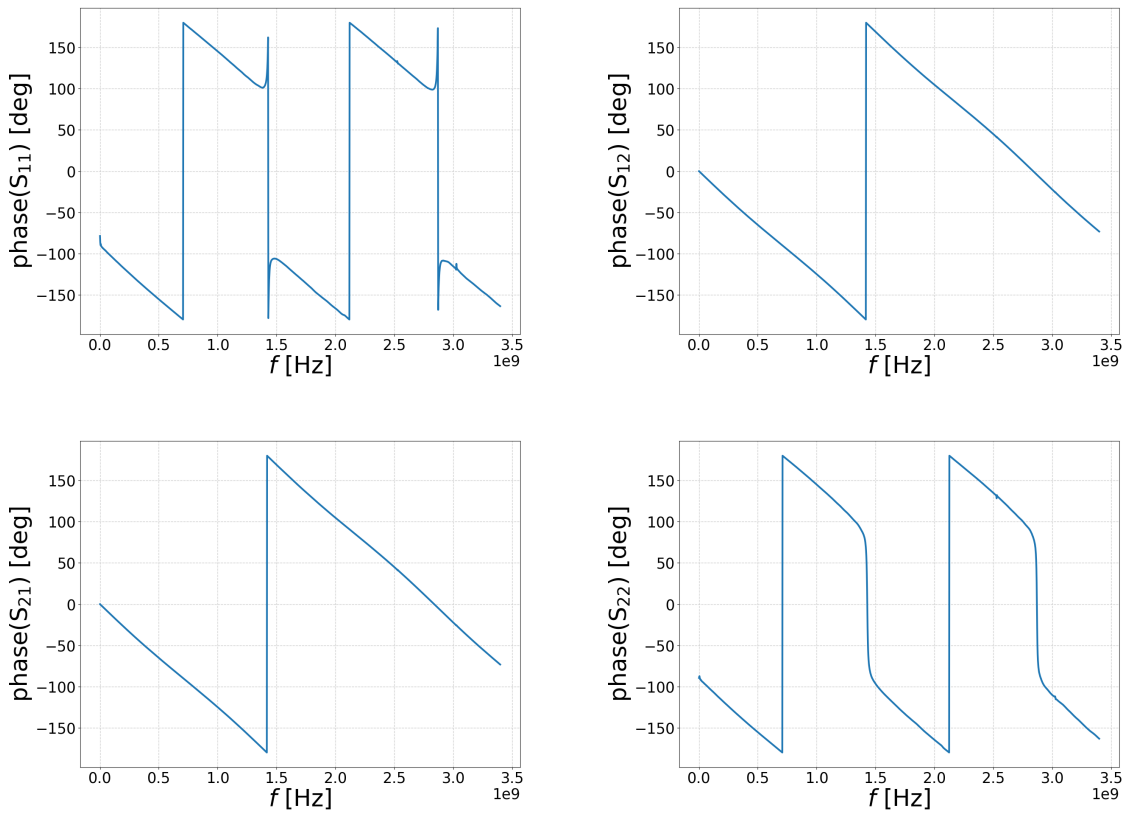


Fig. 19: Results of the phases of all the S-parameters with the measurement with PE. The frequency range is set from 300 kHz to 3.4 GHz with 1601 data points.

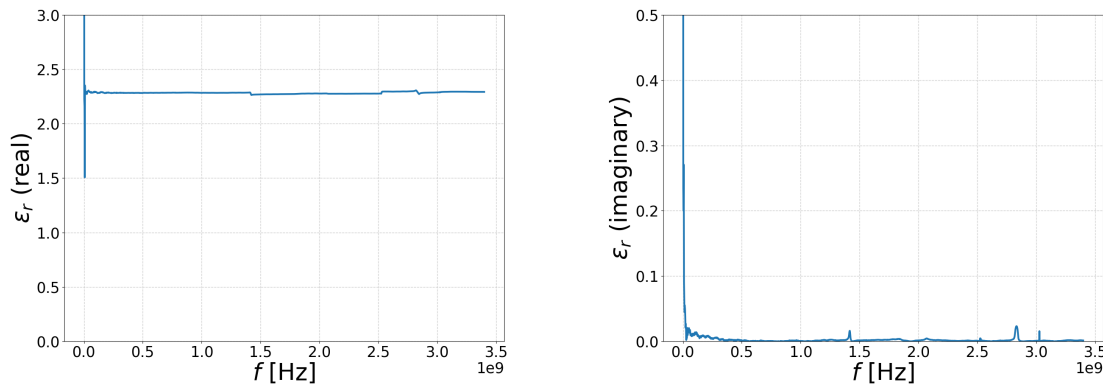


Fig. 20: Reconstructed permittivity of the PE is shown in figure 18. The left graph is displaying the real and right graph the imaginary part of the permittivity.

This section shows the same procedure as the previous section but now for PE. As stated in beforehand, a constant behavior for the real part of the permittivity at a value close to 2.26 is observed. When once again averaging for testing purposes over the same frequency span it becomes a value of 2.28. This is also very close. The Imaginary part here is neglectable.



Fig. 21: Picture of the PE probe which is measured in this section.

3.2.3 PVDF (Polyvinylidenfluorid)

PVDF is another synthetic for which the S-parameters are measured. This is the first and only synthetic taken into consideration in this thesis without a constant permittivity. However there are no literature values found for PVDF in the frequency range of Gigahertz. For an indication what magnitude of a relative permittivity is to be expected, there are literature values in a range of up to 10 Megahertz. In this range the relative permittivity is monotonically decreasing and ending at value of approximately 4 at 10 Megahertz [10, p. 3].

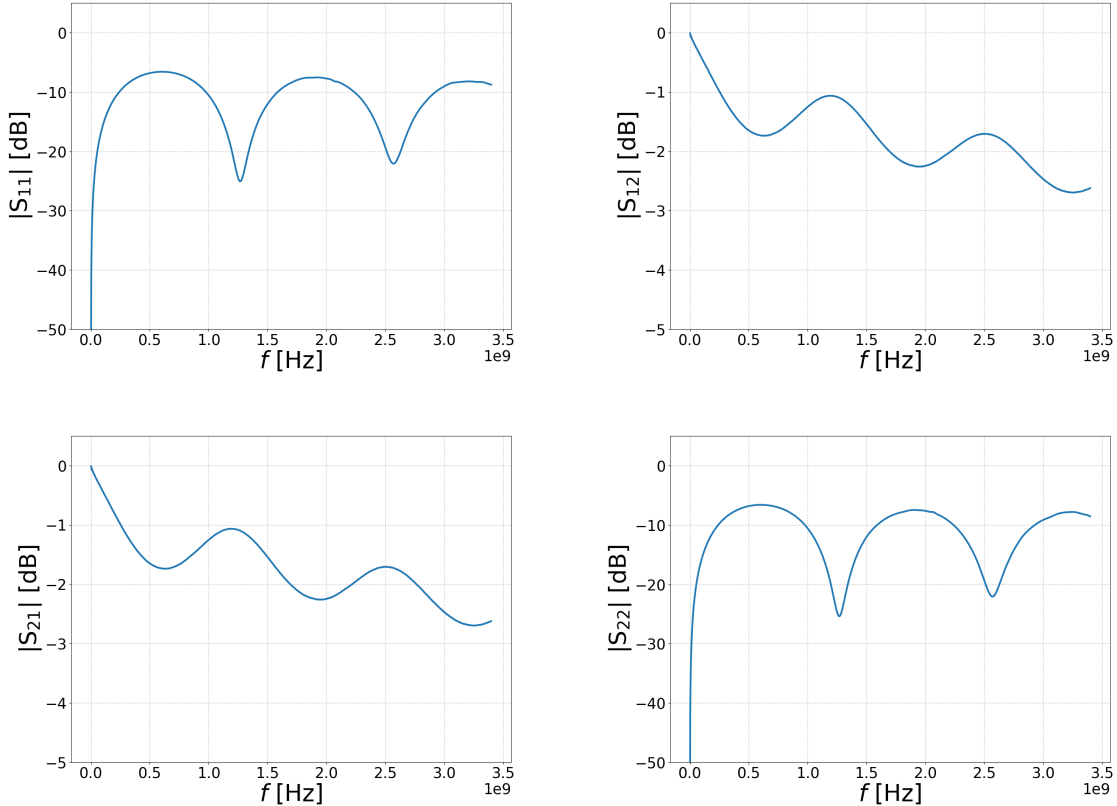


Fig. 22: Results of the absolutes of all S-parameters with the measurement with PVDF. The frequency range is set from 300 kHz to 3.4 GHz with 1601 data points.

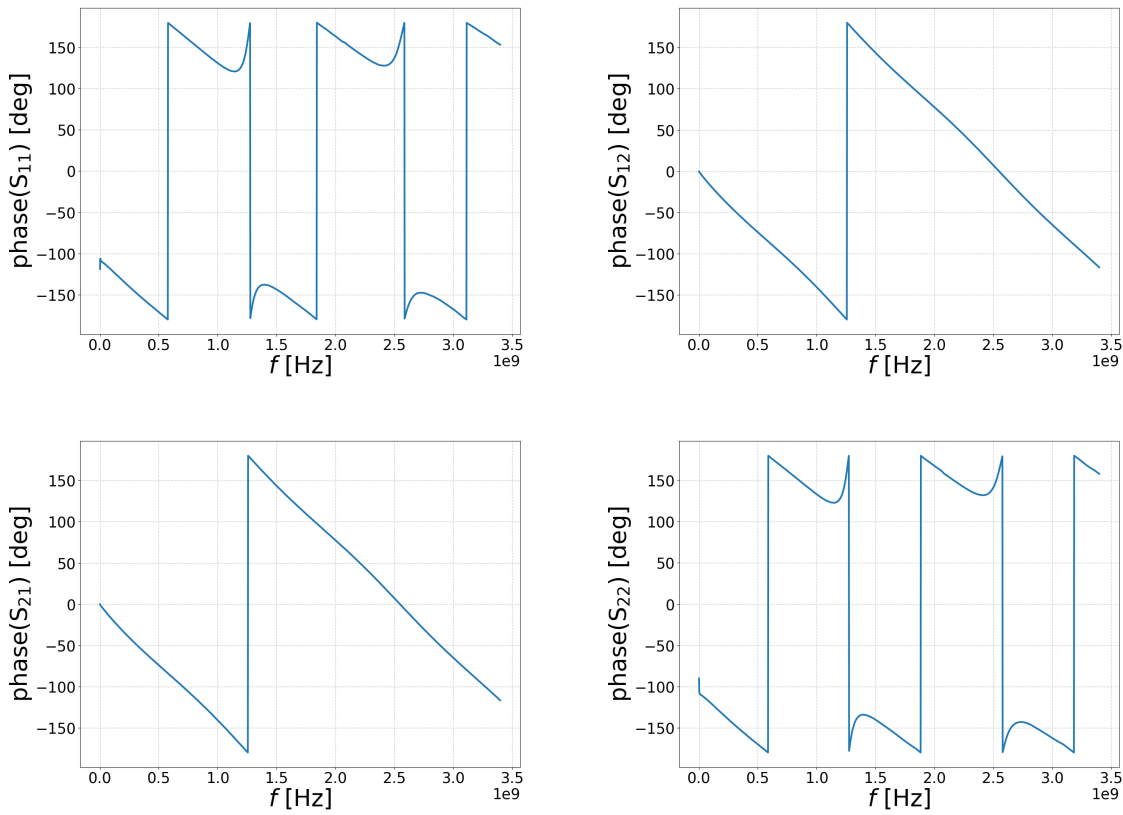


Fig. 23: Results of all the phases of the S-parameters with the measurement with PVDF. The frequency range is set from 300 kHz to 3.4 GHz with 1601 data points.

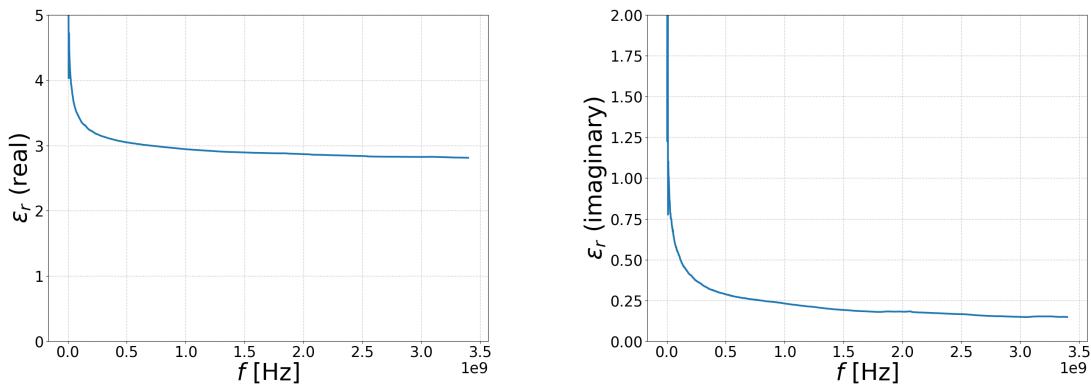


Fig. 24: Reconstructed permittivity of the S-parameters of PVDF shown in figure 22. The left graph is showing the real and right graph the imaginary part of the permittivity.

This section displays the graphs analogue to a manner in the previous sections. The transmitting S-parameters appear very symmetrical to each other as well as the reflecting parameters. The real permittivity is monotonically decreasing and the imaginary part is noticeable.



Fig. 25: Picture of the PVDF probe which is measured in this section.

4 Conclusion and Future Applications

The goal of this thesis is to present a working method for reconstructing the relative permittivity in a broadband frequency range. When taking the results of the simulation into consideration this goal had been archived accurately. When comparing the results of PTFE and PE, there is a small difference to the expected values. However due to the real life application in the evaluation there is a mistake to be expected in the process of the measurement itself. The two port measurement of the VNA has by default various error sources which have to be corrected by a calibration. Moreover there is the possibility for unwanted air gaps between the DUT and the adapters. Therefore the reason for this variance is expected to be found in the realization of the experiment and not in the analytic reconstruction method.

When considering the utility of this model, one can only reconstruct the permittivity of a homogeneous one layered sample. According to the analytic Method it is however possible to create the expected S-parameters of a multiple set of different homogeneous layers and then it would be possible with a recursive method to reconstruct the permittivity of the multiple layered sample. Meaning when guessing the different permittivities and comparing the simulated S-parameters to the measured S-parameters it is then theoretically possible to reconstruct the permittivity. This would be the case for when the guessed permittivity produces the same S-parameter set as the measured ones.

The initial idea however and future purpose of this model is to create a method for reconstructing the properties of soil samples with the background in environmental research. Reconstructing the permittivity of a soil sample would be a first step for archiving a characterization of the measured soil. Other interesting parameters would be to reconstruct the humidity or porosity of the soil sample.

5 Appendix

This section contains the python code used in this bachelor thesis. One section is for the forward model and one for the inverse model. This is also available at my github: <https://github.com/janzimbelmann>

5.1 Code for the Forward Model

Here is the application of the forward model (section: 2.4.1) for the S-parameter simulation:

```

import numpy as np
import matplotlib.pyplot as plt
import skrf as rf
import argparse
import math

if __name__ == '__main__':
    #initial boundary values:
    start = 300000 #first frequency value
    end = 3400000000 #last frequency value
    steps = 1601 #number of frequency points
    z0 = 50 #reference impedance
    d = 0.07 #length of probe
    c0 = 299792458 #speed of light
    freq= np.linspace(start , end , steps)
    z, omega, gamma = [] , [] , []

#—help information:
parser = argparse.ArgumentParser(description='This program creates the\
    S-parameter set for a set of permittivity. The frequency range\
    is by default set from 300kHz to 3.4GHz. You can parse two\
    arguments for the frequency dependence of the real part of the\
    permittivity. According to those arguments the real part is linearly\
    changing from the starting value. There is an analogue parsing option\
    for the imaginary part. This S-parameter set is stored in a .s2p file.')
#parser:
parser.add_argument('name', type=str, nargs='?', default='ntwk',
                    help='Name of the file.')
parser.add_argument('real0', type=float, nargs='?', default=2.1,
                    help = 'starting value of the real part of the permittivity.')
parser.add_argument('real1', type=float, nargs='?', default=2.1,
                    help = 'ending value of the real part of the permittivity.')
parser.add_argument('imag0', type=float, nargs='?', default=0.0001,
                    help = 'starting value of the imaginary part of the permittivity.')
parser.add_argument('imag1', type=float, nargs='?', default=0.0001,
                    help='ending value of the imaginary part of the permittivity.')

```

```

args = parser.parse_args()
eps = np.linspace(args.real0+ args.imag0 *1j , args.real1+args.imag1*1j , steps)

#application of the forward algorithm:
MatrixL = np.matrix([[1,1],[1/z0, -1/z0]])
MatrixR = np.matrix([[1,1],[1/z0, -1/z0]])
S11, S12, S21, S22 = np.array([]), np.array([]), np.array([]), np.array([])
SFull = []
for i in range(steps):
    z.append(z0/np.sqrt(eps[i]))
    omega.append(freq[i] * 2 * np.pi)
    gamma.append(1j * omega[i]/c0*np.sqrt(eps[i]))
    m11 = np.cosh(d*gamma[i])
    m12 = z[i]*np.sinh(d*gamma[i])
    m21 = (1/z[i])*np.sinh(d*gamma[i])
    m22 = np.cosh(d*gamma[i])
    MatrixP = np.matrix([[m11,m12],[m21,m22]])
    MatrixFull = np.linalg.inv(MatrixL) * MatrixP * MatrixR

    S11 = np.append(S11, MatrixFull.item(2)/MatrixFull.item(0))
    S12 = np.append(S12, 1/MatrixFull.item(0))
    S21 = np.append(S21, 1/MatrixFull.item(0))
    S22 = np.append(S22, MatrixFull.item(2)/MatrixFull.item(0))
    SFull.append([[S11[i],S12[i]],[S21[i],S22[i]]])

#storing data in .s2p file:
ntwk = rf.Network(frequency = freq*10**-9,s=SFull,z0=50, name='Simulation')
rf.write(args.name+'.s2p', ntwk)

#plot
ntwk.plot_s_db()
plt.grid(color='0.8', linestyle = '--', linewidth=1)
plt.show()

```

5.2 Code for the Inverse Model

Here is the application of the inverse model (section: 2.4.2) for the complex permittivity reconstruction.

```

import matplotlib.pyplot as plt
import numpy as np
import skrf as rf
import argparse
import math

if __name__ == "__main__":
    #--help information
    parser = argparse.ArgumentParser(description='This program reconstructs\
        the relative permittivity for a S-parameter set of an .s2p file.\
        The display range of the x-axis is configurable by the parser\
        and the default settings might not have the scope of interest.\
        Only the maximum can be changed and the minimum is fixed at 0.')
    #parser
    parser.add_argument('name', type=str, nargs='?', default='ntwk.s2p',
                        help='Name of the file.')
    parser.add_argument('epsrrange', type=float, nargs='?', default=3,
                        help='Range of real epsilon. From zero to variable.')
    parser.add_argument('epsirange', type=float, nargs='?', default=0.002,
                        help='Range of imaginary epsilon. From zero to variable.')
    args = parser.parse_args()
    network = rf.Network('./'+args.name)

    #initial values
    steps = len(network.s) #amount of frequency points
    freq = network.f #frequency
    z0 = 50 #reference impedance
    c0 = 299792458 #speed of light
    d = 0.07 #length of probe
    omega = [] #angular frequency
    S11, S12 = np.array([]), np.array([])
    S21, S22 = np.array([]), np.array([])
    SFull = []
    gammaReal, gammaImag = [], []
    gammaImagCor, gamma = [], np.array([])
    eps = np.array([])

    #application of the inverse algorithm
    for i in range(steps):
        omega.append(2*np.pi*freq[i])

```

```

S11 = np.append(S11, network.s[i][0][0])
S12 = np.append(S12, network.s[i][0][1])
S21 = np.append(S21, network.s[i][1][0])
S22 = np.append(S22, network.s[i][1][1])
SFull.append([[S11[i], S12[i]], [S21[i], S22[i]]])

A = 1+S11[i]
B = (1-S11[i])/z0
C = S12[i]
D = S12[i]/z0

beta = ((A*B)+(C*D))/((A*D)+(B*C))
gammaCalc = np.arccosh(beta)/d
gammaReal.append(np.real(gammaCalc))
gammaImag.append(abs(np.imag(gammaCalc)))

#correction of the wrapping
if(i>0):
    plus = gammaImagCor[i-1] + abs(gammaImag[i]-gammaImag[i-1])
    gammaImagCor.append(plus)
else:
    gammaImagCor.append(gammaImag[i])

for i in range(steps):
    gamma = np.append(gamma, gammaReal[i]+1j*gammaImagCor[i])
    epsAppend = ((c0 * gamma[i])/(1j*omega[i]))**2
    eps = np.append(eps, epsAppend)

#plot
plt.figure(0)
plt.xlabel('$f$ [Hz]')
plt.grid(color='0.8', linestyle = '--', linewidth=1)
plt.plot(freq, np.real(eps))
plt.ylabel('$\text{real}(\epsilon_r)$')
plt.ylim(0,args.epsrange)

plt.figure(1)
plt.xlabel('$f$ [Hz]')
plt.grid(color='0.8', linestyle = '--', linewidth=1)
plt.plot(freq,np.absolute(np.imag(eps)))
plt.ylabel('$\text{imag}(\epsilon_r)$')
plt.ylim(0,args.epsirange)

plt.show()

```

References

- [1] IEEE Standards Board. Ieee standard definitions of terms for radio wave propagation. *IEEE Std 211-1997*, pages i–, 1998.
- [2] J Baker-Jarvis. Transmission/reflection and short circuit line permittivity measurements. *NASA STI/Recon Technical Report N*, 07 1990.
- [3] Inder Bahl. *Lumped Elements for RF and Microwave Circuits*. 2003.
- [4] Picture from: 'Wikipedia'. File:Line model Heaviside.svg — Wikipedia, the free encyclopedia. <http://en.wikipedia.org/w/index.php?title=File%3ALine%20model%20Heaviside.svg&oldid=833294017>, 2019. [Online; accessed 04-March-2019].
- [5] Felix Schmidt. Measuring and modeling dielectric properties along tem waveguides for determination of soil water content, 2013.
- [6] A. G. Gorriti and E. C. Slob. A new tool for accurate s-parameters measurements and permittivity reconstruction. *IEEE Transactions on Geoscience and Remote Sensing*, 43(8):1727–1735, Aug 2005.
- [7] A. M. Niknejad. Calibrating the e5071c network analyzers. <http://rfic.eecs.berkeley.edu/142/labs/resources/Calibration.pdf>, 2019. [Online; accessed 30-Mai-2019].
- [8] D. F. Williams, J. C. M. Wang, and U. Arz. An optimal vector-network-analyzer calibration algorithm. *IEEE Transactions on Microwave Theory and Techniques*, 51(12):2391–2401, Dec 2003.
- [9] W. Barry. A broad-band, automated, stripline technique for the simultaneous measurement of complex permittivity and permeability. *IEEE Transactions on Microwave Theory and Techniques*, 34(1):80–84, Jan 1986.
- [10] C V. Chanmal. Dielectric relaxations in pvd/batio3 nanocomposites. *Express Polymer Letters - EXPRESS POLYM LETT*, 2:294–301, 03 2008.

